https://doi.org/10.5194/egusphere-2024-3579
Preprint. Discussion started: 26 November 2024

Spatially separate production of hydrogen oxides and nitric oxide in lightning

Jena M. Jenkins[1], William H. Brune[1]

[1]Department of Meteorology and Atmospheric Science, Pennsylvania State University, University Park, PA, 16802, USA

Correspondence to: Jena M. Jenkins (jzj76@psu.edu)

Abstract. The atmosphere's most important oxidizer, the hydroxyl radical (OH), is generated in abundance by lightning, but the contribution of this electrically generated OH (LOH) to global OH oxidation remains highly uncertain. Part of this uncertainty is due to the abundant nitric oxide (NO) also generated in lightning, which could rapidly remove the LOH before it can oxidize other pollutants in the atmosphere. However, evidence from a previous laboratory study indicated LOH is not immediately consumed by NO, possibly because LOH's production is spatially separated from the NO production in lightning flashes. This hypothesis of spatially separate OH and NO production is further tested here in a series of laboratory experiments, where the OH decays were measured from spark discharges in air which had increasing amounts of NO added to it. The LOH decayed faster as more NO was added to the air, indicating that the LOH was reacting with the added NO, and not the spark NO. Thus, LOH from lightning flashes is not immediately consumed by the electrically generated NO but is available to oxidize other pollutants in the atmosphere and contribute to global OH oxidation. Subsequent modelling of the laboratory data also supports the spatially separate production of LOH and NO, and further suggests that substantial HONO is also produced by sparks and lightning in the atmosphere.

1 Introduction

Lightning and other electrical discharges have been shown to directly generate extreme amounts of the atmosphere's primary oxidant, the hydroxyl radical (OH), and the closely related hydroperoxyl radical (HO_2) in field studies (Brune et al. 2021; Brune et al., 2022), laboratory studies (Jenkins et al. 2021; Ono and Oda, 2002), and modelling studies (Bhetanabhotla et al., 1985; Ripoll et al. 2014). However, the exact contribution of electrical discharges to global atmospheric OH is highly uncertain. The frequency, duration, and location of weaker electrical discharges, like streamers or corona, are not well known, complicating attempts to estimate global OH production from these discharge types.

In comparison, we know that lightning flashes occur at a rate of 44 s^{-1} (Christian et al., 2003), last <1 second (Rakov and Uman, 2006), and can detect when and where they occur with satellites and lightning mapping arrays, but the extreme amount of nitrogen oxide (NO) also generated in lightning makes estimating the impact of lightning generated OH and HO_2 (hydrogen oxides or HO_x) difficult, as theoretically this NO could rapidly remove the extreme OH before it oxidizes other chemical species in the atmosphere, such as methane, carbon monoxide, sulfur dioxide, or other pollutants. However, evidence from a previous laboratory study suggests that electrically generated HO_x (LHO_x) is not immediately destroyed by electrically generated NO (LNO). In Jenkins et al. (2021), LHO_x generated from a laboratory spark was measured decaying over the course of 100s of milliseconds, while a modelled decay generated with a photochemical box model, the Framework for 0-D Atmospheric Modelling (F0AM) (Wolfe et al., 2016) with the Master Chemical Mechanism v3.3.1 (Jenkin et al., 2015), found that all LHO_x should decay away in less than 10 ms with the extreme LNO simultaneously generated. This discrepancy between the laboratory and model decays suggests that either LHO_x and LNO generation are spatially separated in the spark or some chemistry is missing or incorrect in the model.

Spatially separate production is possible due to the structure of and different types of energy present in lightning flashes and sparks. At the center of a lightning flash is a ~1-2 cm diameter core (Rakov and Uman, 2006) with temperatures exceeding 30,000K (Orville, 1968a). Surrounding this hot core is a weaker and cooler area of electrical discharge, called the corona sheath, extending radially several meters from the hot core (Rakov and Uman, 2006). Some of the radiation emitted by lightning flashes is in the ultraviolet (UV) range, composed of both broad spectrum and line emissions (Orville, 1968b), and including wavelengths <300 nm that are emitted from the sun but normally not present in the troposphere due to their absorption in the higher levels of the atmosphere by ozone. The reach of the UV radiation depends on the wavelength and scattering the radiation encounters but can be as much as 10s of meters. Sparks are essentially a smaller scale version of lightning flashes, still composed of a hot core (though not as hot as lightning) surrounded by a weaker and cooler corona sheath and emitting UV radiation (though not as much as lightning).

The high temperatures of the lightning flash or spark are required to dissociate stable N_2 and make the extreme amounts of NO present in lightning flashes (Chameides et al., 1977), but large amounts of HO_x can also be made by combustion at high temperatures (Dyer and Crosley, 1982). Corona can make extreme HO_x through multiple pathways (Bruggeman and Schram, 2010) while making orders of magnitude less LNO than lightning or sparks (Rehbein and Cooray, 2001). UV radiation can also make extreme OH while making little to no NO by directly dissociating water vapor at wavelengths <200 nm, producing HO_x in two steps:

$$H_2O + hv \rightarrow OH + H \qquad \text{(R1)}$$

$$H + O_2 + M \rightarrow HO_2 + M \qquad \text{(R2)}$$

Thus, with the NO production mostly contained to the hot core but the HO_x production occurring both in the hot core and outside in the corona sheath and the UV radiation, spatially separation LHO_x and LNO production is possible.

https://doi.org/10.5194/egusphere-2024-3579
Preprint. Discussion started: 26 November 2024

To further test the hypothesis that LHO_x and LNO production are spatially separated in spark discharges, a series of laboratory experiments were conducted, as suggested by a previous reviewer, where the LOH and LHO_2 decays from spark discharges in air were measured with different amounts of background NO added into the air flow, from 0 ppbv up to 1000 ppbv of added NO. The decays from the laboratory experiments are also compared to decays calculated by F0AM with MCM to see if the model can successfully reproduce these decays. If LHO_x decays faster as the background NO mixing ratio is increased, then LHO_x is mostly or entirely reacting with background NO instead of spark LNO, confirming that LHO_x and LNO generation is spatially separated in the spark. Otherwise, if the LHO_x decays are unaffected by the amount of added NO, then LHO_x is mostly or entirely reacting with spark LNO, LHO_x and LNO are likely generated in the same location, and some unaccounted-for chemistry is causing the discrepancy between model and measurement.

2 Methods

2.1 Laboratory Experimental Setup

The laboratory setup was nearly identical to the setup used in our previous LHO_x studies (Jenkins et al. 2021; Jenkins and Brune, 2023). Purified and dried air was flowed through a bubbler to add a controlled amount of water vapor, then mixed with dry air that flowed down a quartz (previously Pyrex®) tube (50 mm OD x 46 mm ID x 105 cm) at 50 standard liters per minute, through spark discharges, and over to instruments for measuring OH and HO_2 (Ground-based Tropospheric Hydrogen Oxides Sensor [GTHOS; Faloona et al., 2004]), NO-NO_2-NO_x (ECO PHYSICS nCLD 855Y), and O_3 (Kalnajs & Avallone, 2010). A solid state Tesla coil (Eastern Voltage Research, Plasmasonic® 1.3) was used to generate the sparks across a 0.7 cm gap between tungsten wire electrodes (0.10 cm diameter) inside the flow tube. The sparks were generated in packets of 10 sparks, as signals from individual sparks were too narrow to consistently measure even at the 5Hz sampling rate of GTHOS. Each electrode was attached to a copper rod; one copper rod was attached via a copper wire cable to the output toroid of the Tesla coil, while the other was attached to an electrical ground. All discharges were generated using the same Tesla coil settings. Pressure (MKS Baratron® Type 222) was monitored ahead of the inlet for GTHOS and the Teflon tubing leading to the NO_x and O_3 analyzers, temperature was measured both before air entered the flow tube (Vaisala HMT310) and as the air exited (thermistor), and the water vapor mixing ratio (Vaisala HMT310) was also measured before the air entered the flow tube. The air velocity was measured with an anemometer (TSI Inc., 8455-09) before running experiments, and the flow in the tube was previously determined to be laminar that is not fully developed (Jenkins et al., 2021). The absolute uncertainty and limit of detection at the 68% confidence level was ±20% and ~1 pptv for the HO_x measurements from GTHOS, ±10% and ~1–3 ppbv for the NO_x measurements, and ±5% and ~20 ppbv for the O_3 measurements.

The experiments were conducted as follows. To capture the LHO_x decay, the copper rods were moved so discharges were generated in 5 different positions in the flow tube. By moving the discharge, the distance between the discharge and instrument inlets was changed, which also changed the time between the LHO_x generation and measurement, producing the LHO_x decay over time. The different amounts of added NO in the system were created by adding NO (Linde, 4.83 ppm) to the air flow before it entered the flow tube to create mixing ratios of 0, 50, 100, 250, 500, or 1000 ppbv (all within ± 6%). Data were collected at pressures of 970 hPa, 770 hPa, 570 hPa, and 360 hPa (all within ± 2%), water vapor mixing ratios between 2000-2400 ppmv, and temperatures between 289-294K.

Normally GTHOS uses two detection axes to simultaneously measure OH and HO_2, but only one detection axis was available when these experiments were conducted. To obtain both OH and HO_2 measurements for these experiments, OH was measured in a set of experiments, and total HO_x was measured in another set of experiments conducted under the same conditions. The average OH measured at each position was subtracted from the total HO_x generated at the same position and collected under the same conditions to determine the HO_2 generated.

2.2 Laboratory Data Processing

Each spark discharge created a spike in the OH, HO_2, NO, and NO_x signals. No O_3 was detected in these experiments. These spikes were integrated over time to determine the total amount of chemical generated by the spark discharge. From previous tests, only about 85% of the generated LNO_x is sampled (Jenkins et al., 2021), so the LNO and LNO_2 results were corrected up 15% to account for the LNO_x that is not sampled. OH and HO_2 have similar diffusion coefficients to NO_x, so OH and HO_2 were also corrected up 15% to account for sampling. Additionally, the lifetime of NO_x is long relative to the time it spends in the flow tube (hours vs <0.5 seconds, respectively), so any change in the NO_x mixing ratio across the different positions was assumed to come from diffusion and not chemical loss. The LOH and LHO_2 measurements were also corrected up based on the NO_x diffusion to account for diffusion losses.

Both the LOH and LHO_2 decays were fitted with equations assuming constant, first-order losses. These equations were extrapolated back to time-zero to determine the initial amount of these species generated in the discharge. In some experiments, the HO_x decay was fast enough that usable HO_x data was not available at all 5 flow tube positions. If at least 3 positions had clear OH and HO_2 signals, the decay was included in the results; if only 2 positions or less were available, the data were not used in the results, as there was not enough confidence in the extrapolated fit. Consequently, not all pressures have results for all the different amounts of added NO.

The initial LNO_x formed in the discharges was taken as the LNO_x in the position closest to the instrument inlets as it was least affected by diffusion. NO_2 made up <10% of total NO_x.

2.3 Model Setup

The modelling experiments were conducted using F0AM v3 with MCM 3.3.1 chemistry. The laboratory data were collected in 10 spark packets, but the chemical measurements were scaled down to single spark equivalents before inputting them into the model. The reason for scaling down is two-fold. First, even at the slowest speed in the flow tube, one spark will travel ~7 cm before the next one occurs, and previous work has shown that the HO_x and NO_x measurements scale proportionally to the number of sparks in the packet (Jenkins et al., 2021), indicating that the chemicals generated by sparks within a packet are likely not overlapping. Second, due to the nonlinear chemistry between HO_x and NO_x, we cannot assume that any modelling done with 10 sparks will scale simply to a single spark. Therefore, because each spark within a packet can be treated as an independent event, the modelling was done using HO_x and NO_x values scaled down to a single spark.

The initial OH and HO_2 determined from the extrapolation of the laboratory decays, scaled down 10-fold, were chosen as the initial OH and HO_2 (respectively) for the model runs. For NO_x, three cases were tested. In the first case, only the added NO was included in the model, and no spark NO_x was included. In the second case, the added NO plus all the spark NO_x was included, and in the third case, the added NO plus only a small percentage of the spark NO_x was included. The laboratory air was found to contain ~20 ppbv of CO which was also included in all the model experiments, along with wall loss at a rate of 0.9 s^{-1} for OH (no wall loss was observed for HO_2). The model experiments ran for 0.5 seconds of experiment time using the same pressure, temperature, and water vapor as the laboratory experiments, and included no dilution.

3 Results

3.1 Laboratory Results

As an increasing amount of NO was added to the air flow in the laboratory experiments, the OH and HO_2 decays became progressively steeper, as shown Figure 1 (970 hPa and 360 hPa) and Figure S1 (770 hPa and 570 hPa). In other words, both OH and HO_2 decayed faster as more NO was added to the air flow. This dependence of the OH and HO_2 decays on the added NO indicates that LHO_x is reacting mostly with the added NO, and little or not at all with the spark NO_x, supporting the hypothesis that the HO_x we measure from spark and lightning discharges is produced separately from the spark NO_x.

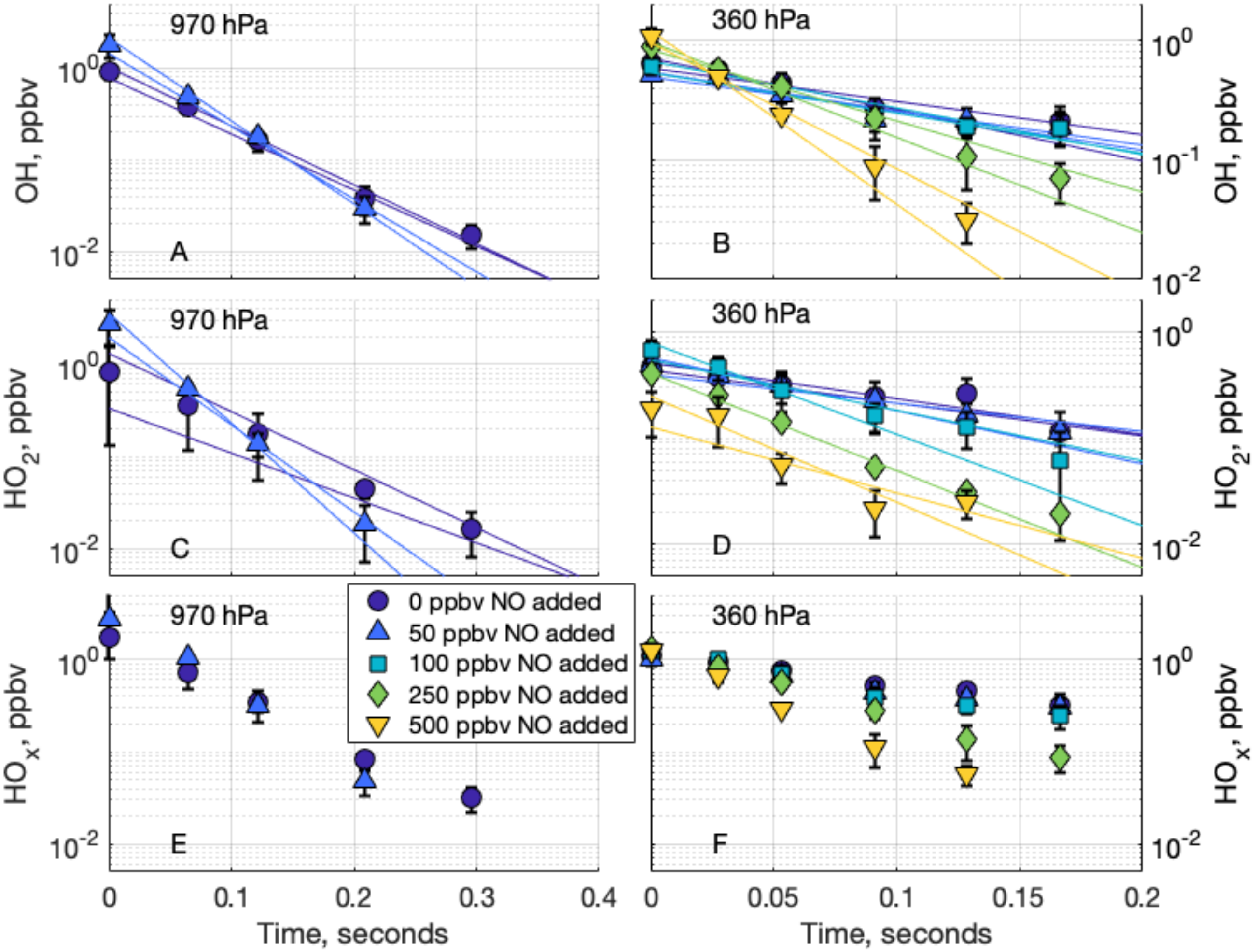

Figure 1: Laboratory decays of OH (A,B), HO_2 (C,D), and net HO_x (E,F) at 970 hPa (A,C,E) and 360 hPa (B,D,F). The markers are the averaged data points measured from 1-2 decays in the laboratory, with the markers at time zero the averaged extrapolated values from the decays. The lines on A, B, C, D are the linear fits to the individual decays. Error bars are the standard deviation from averaging multiple measurements. 155

3.2 Laboratory versus model decays

Comparing the laboratory OH decays to the model decays from F0AM further supports the separate production of LHO_x and LNO, but also indicates that LHO_x and LNO or other chemical products from the spark discharges are likely interacting. For example, at 770 hPa and 0 ppbv of added NO, the laboratory LHO_x measurements decay neither as fast as when 100% of the 160 spark NO_x is added to the model nor as slowly as when no spark NO_x is added to the model (Figure 3A,B). If LHO_x and

LNO_x were generated in the same place, the laboratory LHO_x decays would match the model decay with 100% LNO_x included, and if LHO_x and LNO_x did not interact at all, the laboratory decays would match the 0% LNO_x model case. The laboratory decays falling in between the two model runs indicates that LHO_x is either partially interacting with LNO_x, or it is interacting with some other product(s) from the sparks.

As the background NO was increased, the gap between the laboratory decay and 0% LNO_x model case decreases (Figure 3C,D), and this gap decreases further as more background NO was added (Figure 3E,F). This decrease in the difference between the laboratory and model decays is likely because as the background NO was increased, it accounted for an increasing amount of the HO_x reactivity compared to the spark products. This increasing agreement between the model and laboratory decays as the added NO increased can be seen at 970 hPa, 570 hPa, and 360 hPa as well (Figures S2, S3, S4, respectively), and is another indicator that LHO_x is mostly made separate from the LNO_x made in the spark hot channel.

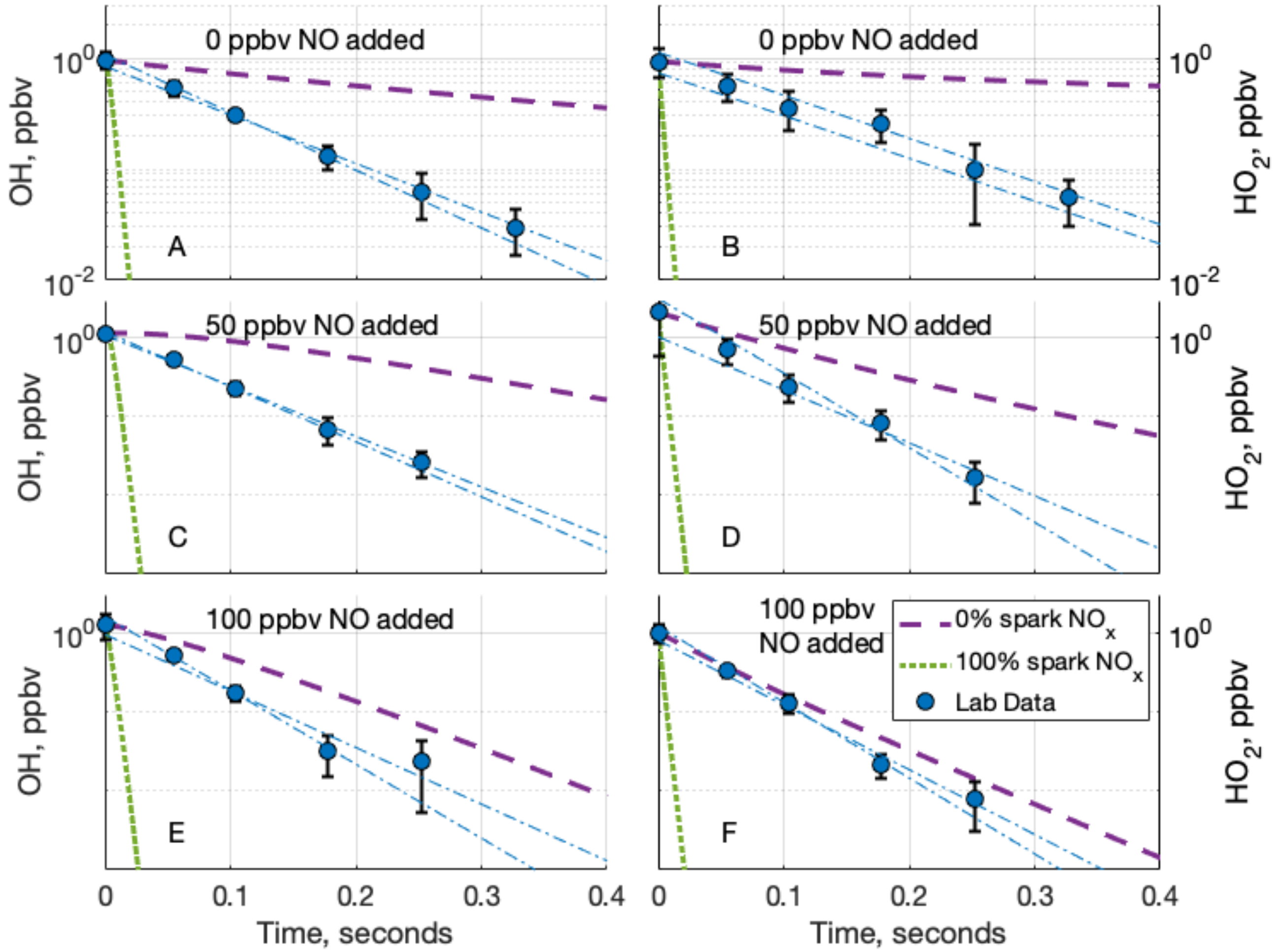

Figure 2: Comparison of measured OH (A,C,E) and HO_2 (B,D,F) laboratory decays and two model decays at 770 hPa and (A,B) 0 ppbv of added NO, (C,D) 50 ppbv of added NO, and (E,F) 100 ppbv of added NO. The dashed purple lines are the model decay with only the added NO, and includes no NO_x from the spark, and the dotted green lines are the model decay with the added NO and all of the spark NO_x. The blue circles are the average laboratory measurements and average extrapolated value at time zero, while the dashed-dotted blue lines are the individual extrapolated linear fits to the laboratory data. Error bars are the standard deviation from averaging multiple measurements.

3.3 Improving the measurement-model agreement

The agreement between the laboratory and model decays is at its worst when 0 ppbv of NO was added in the laboratory experiments. As these cases are also the most relevant to the atmosphere, trying to resolve this disagreement can also give insight into lightning chemistry in the atmosphere.

https://doi.org/10.5194/egusphere-2024-3579
Preprint. Discussion started: 26 November 2024

Previously, the measured-modelled agreement was improved by adding a small amount, 0.5%, of NO_x from the sparks into the model runs, which brought good agreement to both OH and HO_2 (Jenkins et al., 2021). However, the model in the previous study was initialized using the full 10 spark packet data and also did not include the OH wall loss. Here, adding 3% of the spark NO_x to the model brings agreement within uncertainty to the laboratory HO_2 data, but the OH data is still overestimated by the model (Figure S5). Adding 5% (970, 770, and 570 hPa) or 10% (360 hPa) of LNO_x instead brings measured-modelled agreement for OH, but the HO_2 data is then consistently underpredicted by the model (Figure S6). There is no amount of LNO_x that can match the OH and HO_2 measurements simultaneously, leaving some chemistry still unaccounted for in the model.

Adding ~10 s^{-1} of OH reactivity into the model along with 3% LNO_x can resolve the discrepancy (Figure S7) within uncertainty. What chemical species could be responsible for this reactivity? In addition to the HO_x, NO_x and O_3 we measure, many other species are generated in sparks as well, including atoms, ions, and excited states such as O, N, H, N_2^+, $O(^1D)$, O^-, and others; other molecules that are primary products of the discharge, like N_2O and CO; and secondary products formed from reaction between or within the first two categories, like H_2O_2, HONO, and NO_2 (Bhetanabhotla et al., 1985; Boldi, 1992; Ripoll et al., 2014). For one (or more) of these species to account for the missing reactivity, it must fulfill a few criteria. First, its lifetime needs to be long enough so it is still present over the time frame we measure the HO_x decays, at least 0.2-0.5 seconds post-discharge. Second, it needs to react with OH on the same 0.2-0.5 second time frame, so it must either react with OH quickly or be present in large enough quantities to compensate for a slow reaction rate. Third, it must spatially overlap with the LHO_x we measure, so either it is produced in the corona sheath and/or UV radiation, or it is produced in large amounts in the hot core, with ~3% mixing out as we think LNO_x is doing. Lastly, the reaction between OH and this species must not produce HO_2. The mismatch between the model and measurements is because OH is overpredicted by the model relative to HO_2. If the reaction between OH and the missing species yields HO_2, then instead of increasing the OH loss rate, OH will be quickly recycled through the reaction $HO_2 + NO \rightarrow OH + NO_2$.

Neither of the first two categories of species, the atoms, ions, and excited states or the other primary molecules, can account for the missing reactivity in the model. The lifetime of the atoms, ions, and excited states species will be too short to affect the HO_x decays over 0.2-0.5 seconds, failing the first criterion. On the other hand, the primary products CO and N_2O fail the second criterion. Both species are longer lived than the first category, but their reactions with OH are relatively slow, and not enough of these species will be produced to compensate. For example, only about ~340 ppbv of N_2O is expected to be made in the combined hot core and corona sheath of a lightning flash (Brandvold et al., 1989; Brandbold et al., 1996; Donohoe et al., 1977; Hill et al., 1984; Levine et al., 1979), but ~11,000 ppmv would need to be produced in the laboratory sparks to compensate for a reaction rate of k_{N_2O+OH} = 3.8×10^{-17} cm^3 $molecules^{-1}$ s^{-1} (Biermann et al., 1976). The reaction between CO and OH is faster, with k_{CO+OH} =2.3×10^{-13} cm^3 $molecules^{-1}$ s^{-1} at 970 hPa in F0AM, and only ~1.8 ppmv of CO is needed to satisfy the missing reactivity in the model. But this 1.8 ppmv is ~12% of the 14.6 ppmv of CO expected to be made in the lightning hot core (Bhetanabhotla et al., 1985; Levine et al., 1979), and it is unlikely that the laboratory sparks are making as much CO as a lightning flash. The reaction of CO and OH also produces HO_2, leading to OH recycling.

The secondary discharge products are long-lived enough to still exist 0.2-0.5 seconds after the discharge, and their reaction rates with OH are faster than the rates with the primary products, so less of them are required to satisfy the missing reactivity compared to the primary products. Still, modelling results indicate that at most ~400 ppbv of H_2O_2 is generated in the lightning hot channel, and if only 3% of the hot channel mixes out, then this will not be enough to satisfy the ~250 ppbv of H_2O_2 needed to account for the missing OH reactivity in the sparks based on the reaction rate of $k_{H_2O_2+OH}$ = 1.7×10^{-12} cm^3 molecules^{-1} s^{-1} from F0AM. Additionally, the reaction of OH and H_2O_2 produces HO_2. For NO_2, we have already included 3% of what we measure in the laboratory experiments in the model runs, which amounts to <10 ppbv of NO_2.

HONO, however, could account for the missing reactivity. It meets all four of the criteria: it lasts long enough to affect the HO_x decays; its reaction with OH does not recycle HO_x; it can react with OH over the 0.2-0.5 second time frame; and production of HONO in the core is expected to be high enough that only ~3% overlapping from the core could account for the OH reactivity. A model study including HONO production in the hot lightning core suggests as much as 12.6 ppmv of HONO can be generated within 10 ms of the discharge (Bhetanabhotla et al., 1985), and we only need ~70 ppbv of HONO to fulfill the missing reactivity, using the F0AM reaction rate of $k_{OH+HONO}$=6.1×10^{-12} cm^3 molecules^{-1} s^{-1}. Even considering that the laboratory sparks are smaller and cooler than a real lightning flash, substantial HONO production in the range of 1-2 ppmv is very much possible for the laboratory sparks as well.

Chemical models of the hot lightning channel show that both LNO and LOH production is extreme inside the lightning hot channel. For example, the model from Bhetanabhotla et al. (1985) has as much as 4300 ppmv of LNO and 860 ppmv of LOH initially produced, while the simulations of Ripoll et al. (2014) has as much as 42000 ppmv of LNO and 8400 ppmv LOH, with LNO and LOH within an order of magnitude of each other in the shock front. As a test, a model experiment was run assuming 4 ppmv of LNO is initially produced in the laboratory sparks, which is only ~1.4-2 times our laboratory measurements for LNO, along with 2.8 ppmv of hot core LOH and no other chemicals added. The result of this experiment is HONO production in the range of 1-2 ppbv across all pressures (Table 1). Additionally, this HONO is generated fast, before we make our first measurement of HO_x in the laboratory flow tube. All the core LOH is also titrated to <1 pptv (our limit of detection in these experiments) over the same time frame the HONO is generated, so it would not be detected by GTHOS in the laboratory experiments, consistent with our observations. The only model case where the core LOH is not titrated to less <1 pptv before the first laboratory measurement is made is at 360 hPa, but even at this pressure, the model predicts that HONO, NO, and NO_2 are all within 1% of their final values when that first measurement is made.

Table 1. Comparison of the averaged NO and NO_2 measured in the laboratory experiments and the predicted NO, NO_2, and HONO from a model run starting with 4 ppmv of LNO and 2.8 ppmv of LOH.

	970 hPa		770 hPa		570 hPa		360 hPa	
	Lab	Model	Lab	Model	Lab	Model	Lab	Model
NO	1850	1820	1950	1870	2200	1930	2900	2040
NO_2	220	380	140	410	140	440	110	490
HONO	-	1670	-	1590	-	1490	-	1300
Time* (s)	0.064	0.019	0.055	0.027	0.042	0.0384	0.028	0.074

*For the laboratory data, time is when the first HO_x measurement is made post-spark. For the model data, time is when OH has been titrated to <1 pptv, our limit of detection in these experiments.

This model run demonstrates that HONO can be formed fast and in large amounts in the spark discharges. The initial chemistry in the sparks is occurring at thousands of degrees Celsius with electrons and many other chemical species besides NO and OH present, and the production of these species may have spatial dependencies that we cannot incorporate or account for in F0AM. These limitations may explain why the model does not entirely reproduce the NO and NO_2 laboratory measurements. Still, the model results are within an order of magnitude of the laboratory results while simultaneously producing substantial HONO. Adding 3% of the modelled HONO from Table 1 into the model of the laboratory decays drastically improves the agreement between the modelled and measured OH, and in some cases brings the modelled and measured decays into agreement within the laboratory uncertainty (Figure 3). A diagram of the simplified HO_x and NO_x spark chemistry discussed in the preceding paragraphs is shown in Figure 4.

https://doi.org/10.5194/egusphere-2024-3579
Preprint. Discussion started: 26 November 2024

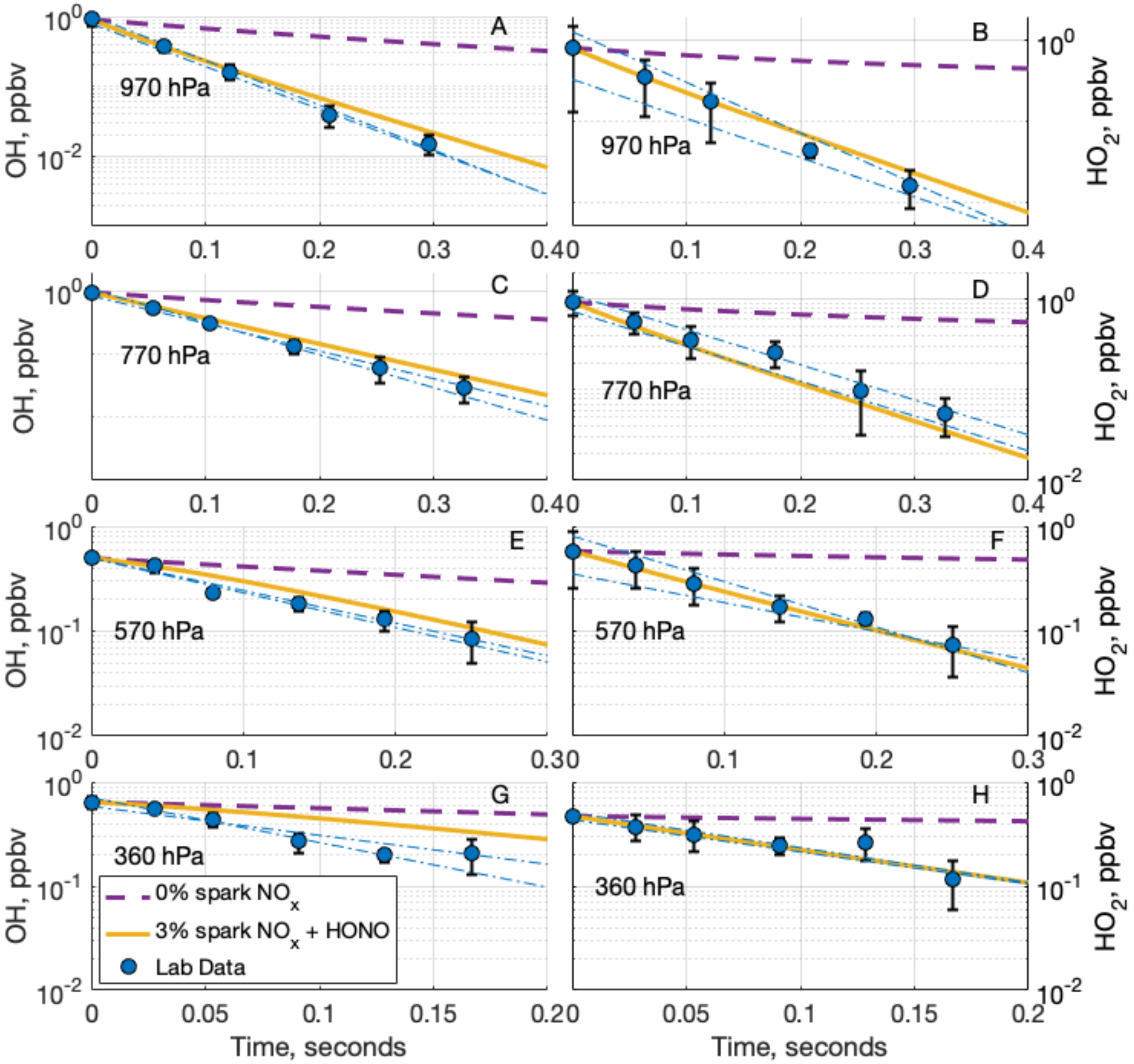

Figure 3: Comparison of measured OH (A,C,E,G) and HO_2 (B,D,F,H) laboratory decays and two model decays at (A,B) 970hP, (C,D) 770 hPa, (E,F) 570 hPa, and (G,H) 360 hPa. The dashed purple lines are the model decay including no NO_x from the spark, and the solid yellow lines are the model decay including 3% the spark NO_x and 3% of the HONO predicted to be generated in a model run. The blue circles are the average laboratory measurements and average extrapolated value at time zero, while the dashed-dotted blue lines are the individual extrapolated linear fits to the laboratory data. Error bars are the standard deviation from averaging multiple measurements.

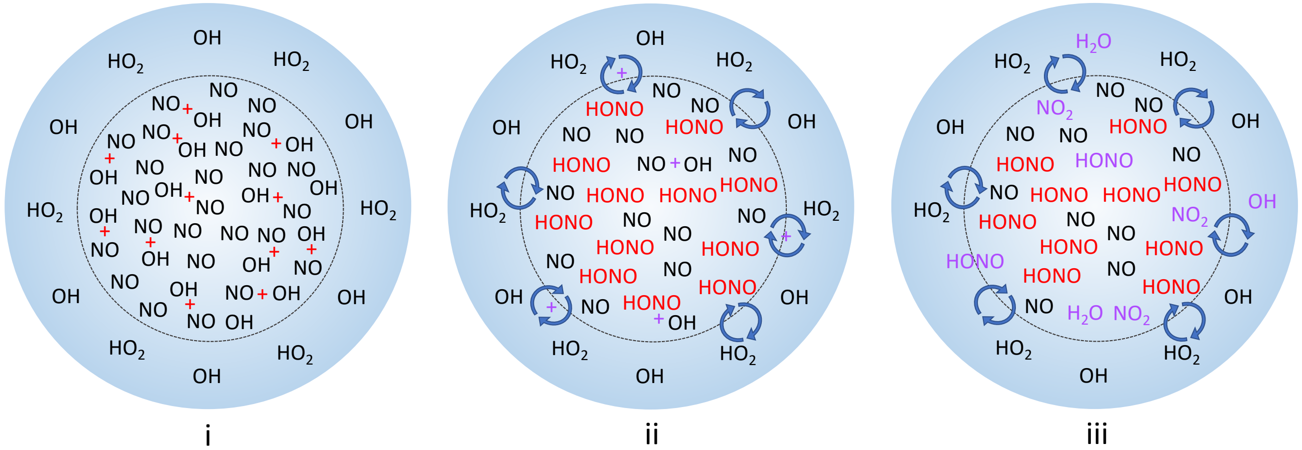

Figure 4: Simplified progression of the HO_x and NO_x chemistry in spark and lightning discharges. (i) Initially, extreme amounts of NO and OH are made inside the lighting hot channel, indicated by the dashed inner circle, while OH and HO_2 are produced outside the hot channel in the corona sheath and UV radiation. (ii) The NO and OH in the hot channel react and form HONO, while the species in the hot channel and corona sheath start to mix together. (iii) Inside the hot channel, any remaining OH reacts with NO and HONO, forming either more HONO or H_2O and NO_2, respectively. Where the hot channel and corona sheath have started mixing, OH and HO_2 from the corona sheath react with NO from the core, forming HONO or OH and NO_2, respectively, while OH from the corona sheath and HONO from the core can also react to form H_2O and NO_2.

4 Conclusions

Both the laboratory and model results confirm that the OH and HO_2 we measure from sparks are likely generated outside the lightning hot channel, separate from the core where the LNO is generated. Note that these results indicate only that the substantial LHO_x *we measure* is generated outside the hot channel; they do not imply that no LHO_x is generated in the hot channel. As stated previously, modelling studies of the lightning hot channel indicate that substantial LHO_x is also generated in the hot channel, likely even more than we measure outside the hot channel. But this hot channel HO_x will be rapidly titrated away in the presence of the large NO also generated in the core, becoming substantial HONO. As for the LHO_x we measure outside the hot channel, LHO_x production has been found to be proportional to ultraviolet radiation (UV) production in corona discharge (Jenkins et al., 2022), and it is likely that UV is also responsible for the LHO_x we measure in sparks and lightning. The consequence of this spatially separate production of LHO_x and LNO is that LHO_x is not immediately consumed by LNO in lightning flashes, but instead is available to oxidize other pollutants in the atmosphere and contribute to global OH oxidation.

Comparing the model and laboratory HO_x decays revealed that substantial HONO is a likely product of our spark discharges, and therefore is also likely to be a substantial product of lightning in the atmosphere. Unfortunately, there is presently little data on electrically generated HONO. Only one modelling study confirms that fast, substantial HONO formation is possible in the aftermath of a lightning flash (Bhetanabhotla et al., 1985); other modelling studies of lightning flash chemistry do not mention HONO, nor are we aware of any laboratory or field studies measuring electrically produced HONO. The Deep Convective Clouds and Chemistry campaign, where the first LHO_x measurements were made in the field, also did not deploy any HONO measuring instruments. Measurements of electrically generated HONO, either in the field or laboratory, would thus be a good target for future work.

Data Availability All data shown in the figures is publicly available at Jenkins and Brune (2024).

Author Contribution Investigation, Methodology, Visualization, Original Manuscript Draft were by JMJ. Funding Acquisition was by WHB. Conceptualization and Reviewing and Editing of the Manuscript were by WHB and JMJ.

Competing Interests The authors declare that they have no conflict of interest.

Acknowledgements We thank P. Stevens for lending us a microchannel plate detector after ours failed.

References

Bhetanabhotla, M. N., Crowell, B. A., Coucouvinos, A., Hill, R. D., and Rinker, R. G.: Simulation of trace species production by lightning and corona discharge in moist air, Atmos. Environ., 19, 1391-1397, doi:10.1016/0004-6981(85)90276-8, 1985.

Biermann, H. W., Zetzsch, C., and Stuhl, F.: Rate Constant for the reaction of OH with N_2O at 298 K, Berich. Bunsen. Gesell., 80, 909-911, doi:10.1021/i160062a006, 1976.

Boldi, R. A.: A model of the ion chemistry of electrified convection, Ph.D. dissertation, Massachusetts Institute of Technology, 1992.

Brandvold, D. K., Martinez, P, and Dogruel, D.: Polarity Dependence of N_2O Formation From Corona Discharge, Atmos. Environ., 23, 1881-1883, doi:10.1016/0004-6981(89)90513-1, 1989.

Brandvold, D. K., Martinez, P., and Hipsh, R. Field measurements of O_3 and N_2O produced from corona discharge, Atmos. Environ., 30, 973-976, doi:10.1016/1352-2310(95)00234-0, 1996.

Bruggeman, P., and Schram, D. C.: On OH production in water containing atmospheric pressure plasmas, Plasma Sources Sci. T., 19, 045025, doi:10.1088/0963-0252/19/4/045025, (2010).

Brune, W. H., Jenkins, J. M., Olson, G. A., McFarland, P. J., Miller, D. O., Mao, J., and Ren, X.: Extreme hydroxyl amounts generated by thunderstorm-induced corona on grounded metal objects, P. Natl. Acad. Sci. USA, 119, e2201213119, doi:10.1073/pnas.2201213119, 2022.

Brune, W. H., McFarland, P. J., Bruning, E., Waugh, S., MacGorman, D., Miller, D. O., Jenkins, J. M., Ren, X., Mao, J., and Peischl, J.: Extreme oxidant amounts produced by lightning in storm clouds, Science, 372, 711-715, doi:10.1126/science.abg0492, 2021.

Christian, H. J., Blakeslee, R. J., Boccippio, D. J., Boeck, W. L., Buechler, D. E., Driscoll, K .T., Goodman, S. J., Hall, J. M., Koshak, W. J., Mach, D. M., Stewart, M. F.: Global frequency and distribution of lightning as observed from space by the Optical Transient Detector, J. Geophys. Res.-Atmos., 108, ACL 4-1-ACL 4-15, doi:10.1029/2002JD002347, 2003.

Donohoe, K. G., Shair, F. H., and Wulf, O. R.: Production of O_3, NO, and N_2O, in a pulsed discharge at 1 atm. Ind. Eng. Chem. Fund., 16, 208-215, doi:10.1021/i160062a006, 1977.

Dyer, M. J., and Crosley, D. R.: Two-dimensional imaging of OH laser-induced fluorescence in a flame, Opt. Lett., 7, 382-384, doi:10.1364/OL.7.000382, 1982.

Faloona, I. C., Tan, D., Lesher, R. L., Hazen, N. L., Frame, C. L., Simpas, J. B., Harder, H., Martinez., M., Di Carlo, P., Ren, X., Brune, W. H.: A laser-induced fluorescence instrument for detecting tropospheric OH and HO_2: Characteristics and calibration, J. Atmos. Chem., 47, 139–167, doi:10.1023/B:JOCH.0000021036.53185.0e, 2004.

Hill, R. D., Rinker, R. G., and Coucouvinos, A.: Nitrous oxide production by lightning, J. Geophys. Res.-Atmos., 89, 1411-1421, doi:10.1029/JD089iD01p01411, 1984.

Jenkin, M. E., Young, J. C., Rickard, A. R.: The MCM v3.3.1 degradation scheme for isoprene, Atmos. Chem. Phys., 15, 11433-11459, doi:10.5194/acp-15-11433-2015, 2015.

Jenkins, J. M., Brune, W. H., and Miller, D. O.: Electrical discharges produce prodigious amounts of hydroxyl and hydroperoxyl radicals, J. Geophys. Res.-Atmos., 126, e2021JD034557, doi:10.1029/2021JD034557, 2021.

Jenkins, J. M., Olson, G. A., McFarland, P. J., Miller, D. O., and Brune, W. H.: Prodigious Amounts of Hydrogen Oxides Generated by Corona Discharges on Tree Leaves, J. Geophys. Res.-Atmos., 127, e2022JD036761, doi:10.1029/2022JD036761, 2022.

Jenkins, J. M., and Brune, W.H.: Effect of Temperature and Water Droplets on Production of Prodigious Hydrogen Oxides by Electrical Discharges, J. Geophys. Res.-Atmos., 128, e2023JD039362, doi:10.1029/2023JD039362, 2023.

Jenkins, J. M., and Brune, W. H.: Spatially separate production of hydrogen oxides and nitric oxide in lightning, datacommons@psu [dataset], https://doi.org/10.26208/0VND-TQ52, 2024.

Kalnajs, L. E., & Avallone, L. M.: A novel lightweight low-power dual-beam ozone photometer utilizing solid-state optoelectronics. J. Atmos. Ocean. Tech., 27, 869–880, doi:10.1175/2009JTECHA1362.1, 2010.

Levine, J. S., Hughes, R. E., Chameides, W. L., and Howell, W. E.: N_2O and CO Production by electric discharge: Atmospheric implications, Geophys. Res. Lett., 6, 557-559, doi:10.1029/GL006i007p00557, 1979.

Ono, R., and Oda, T. Measurement of hydroxyl radicals in pulsed corona discharge. J. Electrostat., 55, 333–342, doi:10.1016/S0304-3886(01)00215-7, 2002.

Orville, R. E.: A High-Speed Time-Resolved Spectroscopic Study of the Lightning Return Stroke: Part II. A Quantitative Analysis, J. Atmos. Sci., 25, 839-851, doi:10.1175/1520-0469(1968)025<0839:AHSTRS>2.0.CO;2, 1968a.

Orville, R. E.: A High-Speed Time-Resolved Spectroscopic Study of the Lightning Return Stroke: Part I. A Qualitative Analysis, J. Atmos. Sci., 25, 827-838, doi:10.1175/1520-0469(1968)025<0827:AHSTRS>2.0.CO;2, 1968b.

Rakov, V. A, and Uman, M. A.: Lightning: Physics and Effects, Cambridge University Press, ISBN 0-521-03541-4, 687 pp., 2006.

https://doi.org/10.5194/egusphere-2024-3579
Preprint. Discussion started: 26 November 2024

Rehbein, N., and Cooray, V. NO production in spark and corona discharges, J. Electrostat., 51–52, 333–339, doi:10.1016/S0304-3886(01)00115-2, 2001.

400 Ripoll, J.-F., Zinn, J., Jeffrey, C. A., and Colestock, P. L.: On the dynamics of hot air plasmas related to lightning discharges: 1. Gas dynamics, J. Geophys. Res.-Atmos., 119, 9218-9235, doi:10.1002/2013JD020068, 2014.

Wolfe, G. M., Marvin, M. R., Roberts, S. J., Travis, K. R., and Liao, J.: The Framework for 0-D Atmospheric Modeling (F0AM) v3.1, Geosci. Model Dev., 9, 3309–3319, doi:10.5194/gmd-9-3309-2016, 2016.